

Chapter 5

Application and Testing of Diagonal, Partial Third-Order Electron Propagator Approximations

Antonio M. Ferreira, Gustavo Seabra, O. Dolgounitcheva,
V. G. Zakrzewski, and J. V. Ortiz

Department of Chemistry, Kansas State University, Manhattan, Kansas 66506-3701

1. INTRODUCTION

Ionization energies and electron affinities are among the most often sought thermochemical data. The importance of electron binding energies is reflected by their presence in a variety of thermodynamic arguments, including thermochemical cycles of acidity and basicity, complexation energies, and oxidation-reduction reactions. Many spectroscopic methods founded on the photoelectric effect, mass spectrometry, electron scattering, and other techniques measure ionization energies and electron affinities. The precision of these experiments in measuring transition energies often contrasts with the paucity of information they generate on accompanying molecular and ionic structures. Computational means of estimating ionization energies and electron affinities therefore provide indispensable corroborative information on structures, especially as the scope of thermochemical and spectroscopic measurements expands.

Given the ubiquitous character of molecular orbital concepts in contemporary discourse on electronic structure, ionization energies and electron affinities provide valuable parameters for one-electron models of chemical bonding and spectra. Electron binding energies may be assigned to delocalized molecular orbitals and thereby provide measures of chemical reactivity. Notions of hardness and softness, electronegativity,

and other qualitative concepts often appeal to molecular orbitals and their corresponding energies.

While many experimental techniques and the majority of computational strategies focus on the generation of increasingly precise ionization energies and electron affinities, fewer methods emphasize the connection between these electron binding energies and the changes in electronic structure they represent. Because one-electron concepts have a history of generating powerful ordering principles for the formulation of hypotheses about electronic structure, it is desirable to use theoretical techniques that show how to connect electron binding energies to orbitals.

2. ELECTRON PROPAGATOR CONCEPTS

Electron propagator theory [1-11] provides a conceptual and computational foundation for this path of inquiry. First, this theory, which is also known as one-electron Green's function theory or as the equation-of-motion method, provides a rigorous framework for calculations of ionization energies and electron affinities. Second, to each electron binding energy ε_p , electron propagator theory associates a function of the coordinates of a single electron $\phi_p(\mathbf{x})$. Both of these objects are results of solving a pseudoeigenvalue problem,

$$\hat{H}^{\text{eff}} \phi_p(\mathbf{x}) = \varepsilon_p \phi_p(\mathbf{x}). \quad (2.1)$$

A special case of this approach is represented by the Hartree-Fock equations, where the effective operator \hat{H}^{eff} contains the usual kinetic (\hat{T}), nuclear attraction (\hat{U}), Coulomb (\hat{J}), and exchange (\hat{K}) components such that

$$\hat{H}^{\text{eff}} = \hat{F} = \hat{T} + \hat{U} + \hat{J} - \hat{K}. \quad (2.2)$$

Since the \hat{J} and \hat{K} operators depend on the occupied orbitals, the pseudoeigenvalue problem must be solved iteratively until consistency is achieved between orbitals that determine \hat{J} and \hat{K} and those that emerge as eigenfunctions of \hat{H}^{eff} , which in this approximation is known as the Fock operator \hat{F} .

Electron propagator formalism allows for generalizations that include the effects of correlation. Here the pseudoeigenvalue problem has the following structure

$$\left[\hat{F} + \hat{\Sigma}(\varepsilon_p) \right] \phi_p(\mathbf{x}) = \varepsilon_p \phi_p(\mathbf{x}). \quad (2.3)$$

Now the Fock operator is supplemented by the self-energy operator $\hat{\Sigma}(E)$. This operator depends on an energy parameter E and is nonlocal. All

orbital relaxation effects between initial and final states may be included in the self-energy operator, as well as all differences in the correlation energies of these states. As in the Hartree-Fock case, matrix elements of the Fock operator still depend on the charge-bond order density matrix \mathbf{D} (also known as the one-electron density matrix) according to

$$F_{rs} = T_{rs} + U_{rs} + \sum_{tu} \langle rt || su \rangle D_{tu}, \quad (2.4)$$

but \mathbf{D} may pertain to a correlated reference state. The energy dependence of the correlated effective operator \hat{H}^{eff} , where

$$\hat{H}^{\text{eff}}(E) = \hat{F} + \hat{\Sigma}(E), \quad (2.5)$$

indicates that the correlated pseudoeigenvalue problem must also contain iterations with respect to E . A search for electron binding energies requires that a guess energy be inserted into $\hat{H}^{\text{eff}}(E)$, leading to new eigenvalues which may be reinserted into $\hat{H}^{\text{eff}}(E)$ in a cyclic manner until consistency is obtained between the operator and its eigenvalues. Approximations to $\hat{\Sigma}(E)$ may be systematically extended until, in principle, exact ionization energies and electron affinities emerge as $\{\varepsilon_p\}$ values.

Eigenfunctions that accompany these eigenvalues have a clear physical meaning that corresponds to electron attachment or detachment. These functions are known as Dyson orbitals, Feynman-Dyson amplitudes, or generalized overlap amplitudes. For ionization energies, they are given by

$$\begin{aligned} \phi_p(\mathbf{x}_1) = & N^{1/2} \int \Psi_N(\mathbf{x}_1, \mathbf{x}_2, \mathbf{x}_3, \dots, \mathbf{x}_N) \Psi_{N-1,p}^*(\mathbf{x}_2, \mathbf{x}_3, \mathbf{x}_4, \dots, \mathbf{x}_N) \\ & \times d\mathbf{x}_2 d\mathbf{x}_3 d\mathbf{x}_4 \dots d\mathbf{x}_N, \end{aligned} \quad (2.6)$$

where \mathbf{x}_i is the space-spin coordinate of electron i . The Dyson orbital corresponding to the energy difference between the N -electron state Ψ_N and the p -th electron-detached state $\Psi_{N-1,p}$ may be used to calculate cross sections for various types of photoionization and electron scattering processes. For example, photoionization intensities $\{I_p\}$ may be determined via

$$I_p = \kappa |\langle \phi_p | \nabla \chi \rangle|^2, \quad (2.7)$$

where χ is a description of the ejected photoelectron. For electron affinities, the formula for the Dyson orbital reads

$$\begin{aligned} \phi_p(\mathbf{x}_1) = & (N+1)^{1/2} \int \Psi_{N+1,p}(\mathbf{x}_1, \mathbf{x}_2, \mathbf{x}_3, \dots, \mathbf{x}_N, \mathbf{x}_{N+1}) \\ & \times \Psi_N^*(\mathbf{x}_2, \mathbf{x}_3, \mathbf{x}_4, \dots, \mathbf{x}_N, \mathbf{x}_{N+1}) \\ & \times d\mathbf{x}_2 d\mathbf{x}_3 d\mathbf{x}_4 \dots d\mathbf{x}_N d\mathbf{x}_{N+1}. \end{aligned} \quad (2.8)$$

In the Hartree-Fock, frozen-orbital case, the reference state consists of a single determinant of spinorbitals and the final states differ by the addition or subtraction of an electron in a canonical spinorbital. The overlaps between states of unequal numbers of electrons represented by the Dyson orbital formulae reduce to occupied or virtual orbitals which are solutions of the canonical Hartree-Fock equations. Dyson orbitals may also be obtained from configuration interaction wavefunctions. Electron propagator calculations, however, avoid the evaluation of complicated many-electron wavefunctions (and their energies) in favor of direct evaluation of electron binding energies and their associated Dyson orbitals. Note that for correlated calculations, the Dyson orbitals are not necessarily normalized. The pole strength P is given by

$$P_p = \int |\phi_p(\mathbf{x})|^2 d\mathbf{x}. \quad (2.9)$$

In the Hartree-Fock, frozen-orbital case, P_p acquires its maximum value, unity. Final states with large correlation effects are characterized by low pole strengths. Transition intensities, such as those in Eq. (2.7), are proportional to P_p .

3. AN ECONOMICAL APPROXIMATION: P3

Canonical Hartree-Fock orbital energies are a convenient and powerful foundation for estimating the smallest vertical electron binding energies of closed-shell molecules. This approximation, which is based on Koopmans's theorem, is the most often used method for assigning the lowest peaks in photoelectron spectra. However, there are many classes of important molecules for which the Koopmans approximation fails to predict the correct order of final states. Average errors made by this frozen-orbital, uncorrelated method are between 1 and 2 eV for valence ionization energies. More confident assignments require that these errors be reduced.

Perturbative expressions for the self-energy operator can achieve this goal for large, closed-shell molecules. In this review, we will concentrate on an approximation developed for this purpose, the partial third-order, or P3, approximation. P3 calculations have been carried out for a variety of molecules. A tabulation of these calculations is given in Table 5.1.

The original derivation of the P3 method was accompanied by test calculations on challenging, but small, closed-shell molecules with various basis sets [12]. The average absolute error was approximately 0.2 eV

Table 5.1 Recent applications of the P3 method.

Reference molecule or ion	Year	Ref.
borazine	1996	12
azabenzenes	1996	13
dichlorobenzene	1996	14
anthracene, phenanthrene, and naphthacene	1996	15
chlorobenzene	1996	16
sym-tetrazine	1997	17
carbon quadranions	1997	18
small anions	1997	19
acridine, phenazine, and diazaphenanthrene	1997	20
benzopyrenes	1997	21
C_7^{2-}	1998	22
anisole and thioanisole	1998	23
butadiene	1999	24
uracil and adenine	2000	25
naphthalene	2000	26
guanine	2000	27
dicarboxylate dianions	2000	28
double-Rydberg anions	2000	29

for vertical ionization energies below 20 eV. Since 1996, the P3 method has been applied chiefly to the ionization energies of organic molecules. For nitrogen-containing heterocycles, P3 corrections to Koopmans results are essential in making assignments of photoelectron spectra. Correlation corrections generally are much larger for hole states with large contributions from nonbonding, nitrogen-centered functions than for delocalized π levels. Therefore, P3 results often produce a different ordering of the cationic states. The accuracy of P3 predictions generally suffices to make reliable assignments. Several reviews on electron propagator theory have discussed relationships between P3 and other methods [9-11].

The P3 method is generally implemented in the diagonal self-energy approximation. Here, off-diagonal elements of the self-energy matrix in the canonical, Hartree-Fock orbital basis are set to zero. In the P3 approximation, correlation contributions to the Fock matrix (also known as the energy-independent, or constant, part of the self-energy matrix) are ignored. The pseudoeigenvalue problem therefore reduces to separate

equations for each canonical, Hartree-Fock orbital:

$$F_{pp} + \Sigma_{pp}(E) = E \quad (3.1)$$

or

$$\varepsilon_p^{\text{HF}} + \Sigma_{pp}(E) = E. \quad (3.2)$$

Only energy iterations are needed in the diagonal self-energy approximation. For example, $\Sigma_{pp}(E)$ may be evaluated at $E = \varepsilon_p^{\text{HF}}$ to obtain a new guess for E . The latter value is reinserted into $\Sigma_{pp}(E)$ and the process continues until consecutive energy guesses agree to within $0.01 \mu E_h$ of each other. Alternatively, one may use Newton's method for solving the roots of a complicated function such that

$$E - \varepsilon_p^{\text{HF}} - \Sigma_{pp}(E) = 0. \quad (3.3)$$

This procedure requires analytical expressions for $\Sigma_{pp}(E)$ and its derivative with respect to E ; it usually converges in three iterations. Neglect of off-diagonal elements of the self-energy matrix also implies that the corresponding Dyson orbital is given by

$$\phi_p(\mathbf{x}) = P_p^{1/2} \phi_p^{\text{HF}}(\mathbf{x}), \quad (3.4)$$

where the pole strength P_p is determined by

$$P_p = \left[1 - \frac{d\Sigma_{pp}(E)}{dE} \right]^{-1}. \quad (3.5)$$

In the latter expression, the derivative is evaluated at the converged energy. Diagonal self-energy approximations therefore subject a frozen Hartree-Fock orbital $\phi_p^{\text{HF}}(\mathbf{x})$ to an energy-dependent correlation potential $\Sigma_{pp}(E)$.

Diagonal matrix elements of the P3 self-energy approximation may be expressed in terms of canonical Hartree-Fock orbital energies and electron repulsion integrals in this basis. For ionization energies, where the index p pertains to an occupied spinorbital in the Hartree-Fock determinant,

$$\begin{aligned} \Sigma_{pp}^{\text{P3}}(E) &= \frac{1}{2} \sum_{iab} \frac{\langle pi || ab \rangle \langle ab || pi \rangle}{E + \varepsilon_i - \varepsilon_a - \varepsilon_b} + \frac{1}{2} \sum_{aij} \frac{W_{paij} \langle pa || ij \rangle}{E + \varepsilon_a - \varepsilon_i - \varepsilon_j} \\ &+ \frac{1}{2} \sum_{aij} \frac{U_{paij}(E) \langle ij || pa \rangle}{E + \varepsilon_a - \varepsilon_i - \varepsilon_j}, \end{aligned} \quad (3.6)$$

where

$$\begin{aligned}
 W_{\text{p}ij} &= \langle \text{p}a || ij \rangle + \frac{1}{2} \sum_{bc} \frac{\langle \text{p}a || bc \rangle \langle bc || ij \rangle}{\varepsilon_i + \varepsilon_j - \varepsilon_b - \varepsilon_c} \\
 &+ (1 - P_{ij}) \sum_{bk} \frac{\langle \text{p}k || bi \rangle \langle ba || jk \rangle}{\varepsilon_j + \varepsilon_k - \varepsilon_a - \varepsilon_b}
 \end{aligned} \tag{3.7}$$

and

$$\begin{aligned}
 U_{\text{p}ij}(E) &= -\frac{1}{2} \sum_{kl} \frac{\langle \text{p}a || kl \rangle \langle kl || ij \rangle}{E + \varepsilon_a - \varepsilon_k - \varepsilon_l} \\
 &- (1 - P_{ij}) \sum_{bk} \frac{\langle \text{p}b || jk \rangle \langle ak || bi \rangle}{E + \varepsilon_b - \varepsilon_j - \varepsilon_k}.
 \end{aligned} \tag{3.8}$$

Indices i, j, k, \dots (a, b, c, \dots) refer to occupied (virtual) spinorbitals. Each of the terms in Eq. (3.6) may be interpreted in terms of simple concepts. The first term pertains to pair correlation energies in the reference state that are missing in the final state due to removal of an electron from the occupied spinorbital p . Summing these terms over all occupied p and setting $E = \varepsilon_p$ for each term would recover the second-order, perturbative correction to the Hartree-Fock total energy of the reference state. The remaining terms account for orbital relaxation and electron correlation in the final state. When either the i or j indices are equal to p , orbital relaxation is described by excitations of electrons into the now vacant, but previously (that is, in the reference determinant) occupied spinorbital p . To describe electron correlation in the final state in terms of spinorbitals optimized for the reference state, it is crucial to include the second and third terms of Eq. (3.7) as well the terms involving the U intermediates of Eq. (3.8). Note that these terms are second-order in electron interaction and therefore generate third-order terms in the self-energy matrix.

For each ionization energy of index p , evaluation of W elements requires arithmetic operations with an O^2V^3 scaling factor, where O is the number of occupied spinorbitals and V is the number of virtual spinorbitals. For each value of E , the U elements must be reevaluated, but the scaling factor here is only O^3V^2 . Since V is generally much larger than O , the latter steps proceed relatively quickly. A complete set of transformed two-electron integrals is not needed, for the set where all four indices are virtual does not appear in these equations. The largest set of integrals, with one occupied and three virtual indices, is needed only in the first summation of Eq. (3.7). Efficient programs may avoid

the evaluation and storage of these transformed integrals by performing this summation with semidirect algorithms [30].

For electron affinities, where the index p pertains to a virtual spinorbital,

$$\begin{aligned}\Sigma_{pp}^{P3}(E) &= \frac{1}{2} \sum_{aij} \frac{\langle pa||ij\rangle\langle ij||pa\rangle}{E + \varepsilon_a - \varepsilon_i - \varepsilon_j} + \frac{1}{2} \sum_{iab} \frac{W_{piab} \langle pi||ab\rangle}{E + \varepsilon_i - \varepsilon_a - \varepsilon_b} \\ &+ \frac{1}{2} \sum_{iab} \frac{U_{piab}(E) \langle ab||pi\rangle}{E + \varepsilon_i - \varepsilon_a - \varepsilon_b},\end{aligned}\quad (3.9)$$

where

$$\begin{aligned}W_{piab} &= \langle pi||ab\rangle + \frac{1}{2} \sum_{jk} \frac{\langle pi||jk\rangle\langle jk||ab\rangle}{\varepsilon_j + \varepsilon_k - \varepsilon_a - \varepsilon_b} \\ &+ (1 - P_{ab}) \sum_{jc} \frac{\langle pc||ja\rangle\langle ji||bc\rangle}{\varepsilon_i + \varepsilon_j - \varepsilon_b - \varepsilon_c}\end{aligned}\quad (3.10)$$

and

$$U_{piab}(E) = \frac{1}{2} \sum_{cd} \frac{\langle pi||cd\rangle\langle cd||ab\rangle}{E + \varepsilon_i - \varepsilon_c - \varepsilon_d} + (1 - P_{ab}) \sum_{jc} \frac{\langle pj||bc\rangle\langle ic||ja\rangle}{E + \varepsilon_j - \varepsilon_b - \varepsilon_c}.\quad (3.11)$$

These formulae are similar to those for the ionization energy case, but with the roles of occupied and virtual indices being reversed. Interpretation of the terms proceeds in an analogous manner. The first summation in Eq. (3.11) now dominates the arithmetic and storage requirements of the calculation. Its scaling factor is OV^4 and it requires electron repulsion integrals with four virtual indices. Practical calculations generally require a semidirect algorithm for this step.

4. OTHER DIAGONAL APPROXIMATIONS

All second-order terms are retained in the P3 self-energy formulae for ionization energies and electron affinities. There are no differences between the expressions used for ionization energies and electron affinities in the second-order self-energy, which reads

$$\Sigma_{pp}^{(2)}(E) = \frac{1}{2} \sum_{aij} \frac{\langle pa||ij\rangle\langle ij||pa\rangle}{E + \varepsilon_a - \varepsilon_i - \varepsilon_j} + \frac{1}{2} \sum_{iab} \frac{\langle pi||ab\rangle\langle ab||pi\rangle}{E + \varepsilon_i - \varepsilon_a - \varepsilon_b}\quad (4.1)$$

for all p . Diagonal, second-order calculations generally overestimate the exact correlation correction to the Hartree-Fock orbital energy. The absolute values of the ensuing errors are often as large as those of Koopmans's theorem [31].

More satisfactory results are obtained from full third-order calculations [32, 33]. Diagonal elements of the full third-order, self-energy matrix are given by

$$\begin{aligned}\Sigma_{pp}^{(3)}(E) &= \sum_{aij} \frac{\left[W_{paj} + \frac{1}{2}U_{paj}(E)\right] \langle pa||ij \rangle}{E + \varepsilon_a - \varepsilon_i - \varepsilon_j} \\ &+ \sum_{iab} \frac{\left[W_{piab} + \frac{1}{2}U_{piab}(E)\right] \langle pi||ab \rangle}{E + \varepsilon_i - \varepsilon_a - \varepsilon_b} \\ &+ \Sigma_{pp}^{(3)}(\infty).\end{aligned}\tag{4.2}$$

Terms containing the W intermediates no longer contain a factor of $\frac{1}{2}$. The energy-independent, third-order term, $\Sigma_{pp}^{(3)}(\infty)$, is a Coulomb-exchange matrix element determined by second-order corrections to the density matrix, where

$$\Sigma_{pp}^{(3)}(\infty) = \sum_{rs} \langle pr||ps \rangle D_{rs}^{(2)}.\tag{4.3}$$

Third-order results for closed-shell molecules have average absolute errors of 0.6 - 0.7 eV [31]. Transformed integrals with four virtual indices and OV^4 contractions for each value of E are required for the U intermediate, which is needed for ionization energy as well as electron affinity calculations.

Second-order and third-order results often bracket the true correction to $\{\varepsilon_p^{HF}\}$. Three schemes that scale the third-order terms in various ways are known as the Outer Valence Green's Function (OVGF) [8]. In OVGF calculations, one of these three recipes is chosen as the recommended one according to rules based on numerical criteria. These criteria involve quantities that are derived from ratios of various constituent terms of the self-energy matrix elements. Average absolute errors for closed-shell molecules are somewhat larger than for P3 [31].

5. NONDIAGONAL APPROXIMATIONS

For many ionization energies and electron affinities, diagonal self-energy approximations are inappropriate. Methods with nondiagonal self-energies allow Dyson orbitals to be written as linear combinations of reference-state orbitals. In most of these approximations, combinations of canonical, Hartree-Fock orbitals are used for this purpose, i.e.

$$\phi_p^{\text{Dyson}}(\mathbf{x}) = \sum_q C_{pq} \phi_q^{\text{HF}}(\mathbf{x}). \quad (5.1)$$

For normalized Hartree-Fock orbitals, the pole strength reads

$$P_p = \sum_q |C_{pq}|^2. \quad (5.2)$$

Nondiagonal self-energy approximations are usually renormalized in the sense that they contain terms in all orders of electron interaction. For example, the 2p-h Tamm-Dancoff approximation (2ph-TDA) is suitable for qualitative descriptions of correlation (shake-up) final states in inner-valence photoelectron spectra [34]. An extension of this method, known as the third-order algebraic diagrammatic construction [ADC(3)] includes all third-order terms in the self-energy matrix. While it retains the ability of 2ph-TDA to generate a simple description of correlation states, ADC(3) is competitive with OVGF in describing final states where the Koopmans picture is qualitatively valid [8]. A nondiagonal, renormalized extension of the P3 method that retains all second-order, self-energy terms is known as NR2 [35]. For valence ionization energies of closed-shell molecules, NR2 is somewhat more accurate than P3, but it is also applicable to final states with large correlation effects [26, 36]. One pays for the enhanced versatility of these methods with increased arithmetic and storage requirements. The relatively modest demands of NR2 calculations make this approximation an attractive target for algorithmic improvements.

It is also possible to employ highly correlated reference states as an alternative to methods that employ Hartree-Fock orbitals. Multiconfigurational, spin-tensor, electron propagator theory adopts multiconfigurational, self-consistent-field reference states [37]. Perturbative corrections to these reference states have been introduced recently [38].

Another approach of this kind uses the approximate Brueckner orbitals from a so-called Brueckner doubles, coupled-cluster calculation [39, 40]. Methods of this kind are distinguished by their versatility and have been applied to valence ionization energies of closed-shell molecules, electron detachment energies of highly correlated anions, core ionization

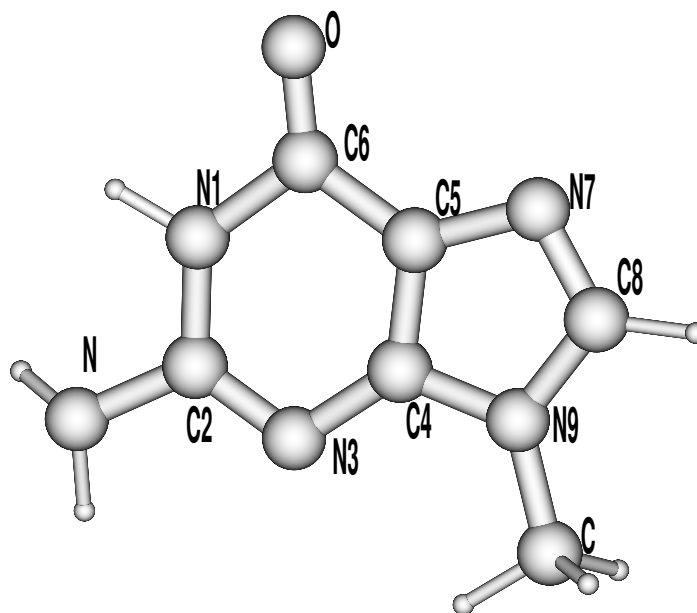


Figure 5.1 The keto form of 9-methylguanine.

energies, and photoelectron spectra of molecules with biradical character [39-43].

6. AN EXAMPLE OF APPLICATION OF P3: 9-METHYLGUANINE

Closed-shell organic molecules are ideal candidates for study with the P3 method for ionization energies. Because of their central position in genetic material as constituents of base pairs, purines and pyrimidines are especially important. The photoelectron spectrum of the purine 9-methylguanine is calculated here as an example of the capabilities of P3 methodology.

Tables 5.2 and 5.3 display vertical ionization energies of the two tautomers (keto and enol) with the lowest energies. The keto form is shown in Fig. 5.1. In the enol form, a proton is transferred from nitrogen 1 to the oxygen atom. P3 ionization energies for both isomers are close to the lowest peak in the photoelectron spectrum (PES) [44].

Table 5.2 Ionization energies (eV) of the keto tautomer of 9-methylguanine.

MO	KT	P3	PES ^a
π_1	8.01	7.98	8.02
π_2	10.57	9.68	9.6
$\sigma_+(\text{N},\text{O})$	11.59	9.68	9.6
$\sigma_-(\text{N},\text{O})$	11.93	9.91	10.3
π_3	11.64	10.39	10.3
π_4	12.44	11.03	10.86
$\sigma_- \text{N}$	13.30	11.34	11.32
π_5	14.75	13.14	13.3

^a Ref. 44.

Table 5.3 Ionization energies (eV) of the enol tautomer of 9-methylguanine.

MO	KT	P3	PES ^a
π_1	8.08	8.05	8.02
π_2	10.18	9.36	9.6
σN	11.26	9.55	9.6
π_3	11.75	10.43	10.3
σN_+	12.38	10.46	10.3
π_4	11.88	10.68	10.86
σN	13.72	11.71	11.32
π_5	14.87	13.31	13.3

^a Ref. 44.

Dyson orbitals in Figs. 5.2 and 5.3 are distributed similarly in the two tautomers.

A more intense peak at 9.6 eV has several constituent ionization energies corresponding to σ and π holes. Large redistributions of the corresponding Dyson orbitals preserve phase relationships and nodal structure in the π_2 case. The structure of the lowest σ Dyson orbital is preserved between the two tautomers, except for the suppression of the nonbonding lobes on nitrogen 1 or on the oxygen, the positions where the shifting proton may reside. For the feature at 10.3 eV, which has an intensity comparable to the one at 9.6 eV, combinations of σ and π holes also pertain. The order of the π_3 and the second σ hole states changes between the two isomers. There are substantial changes in the

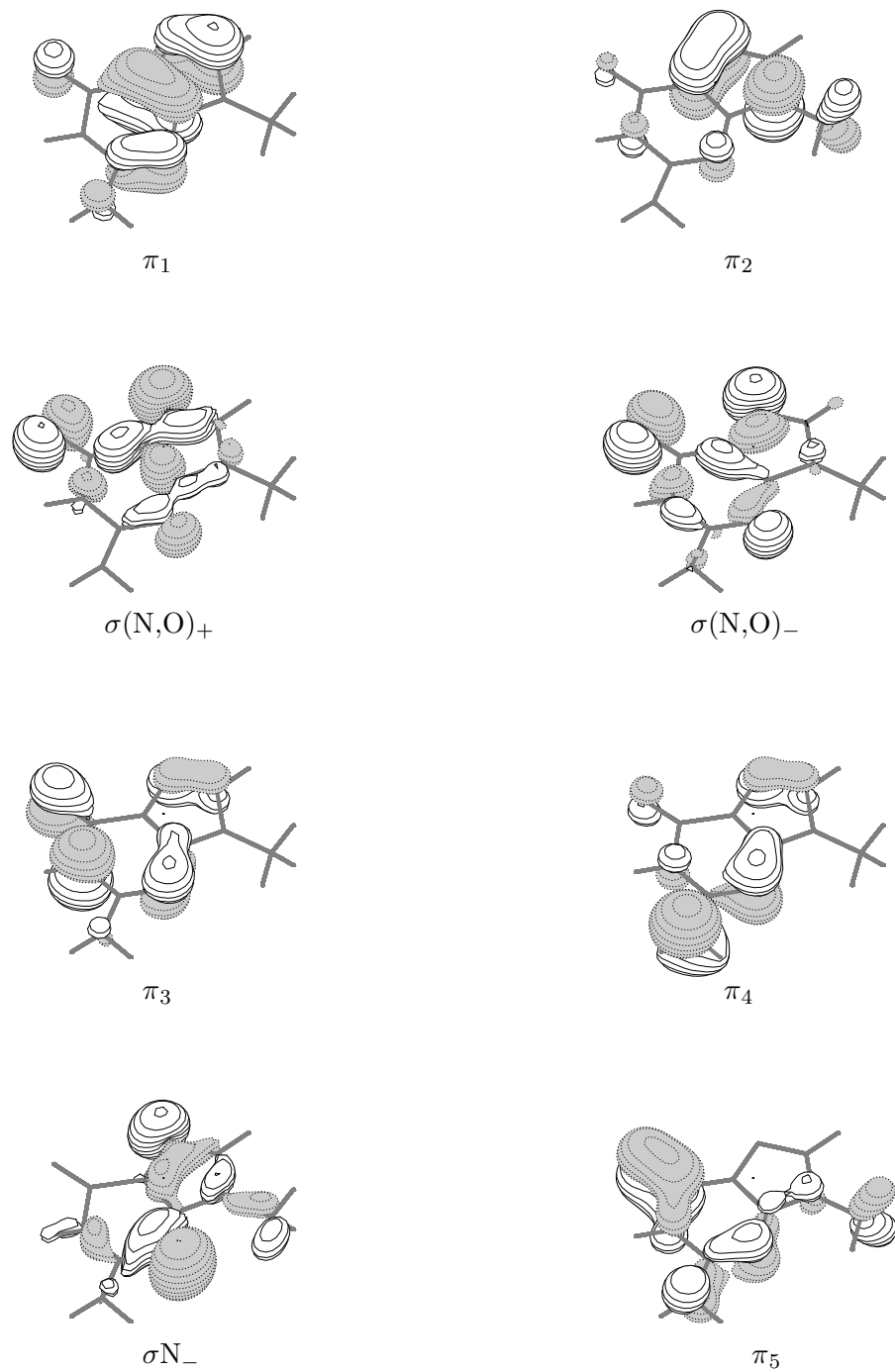


Figure 5.2 Dyson orbitals of the keto form of 9-methylguanine.

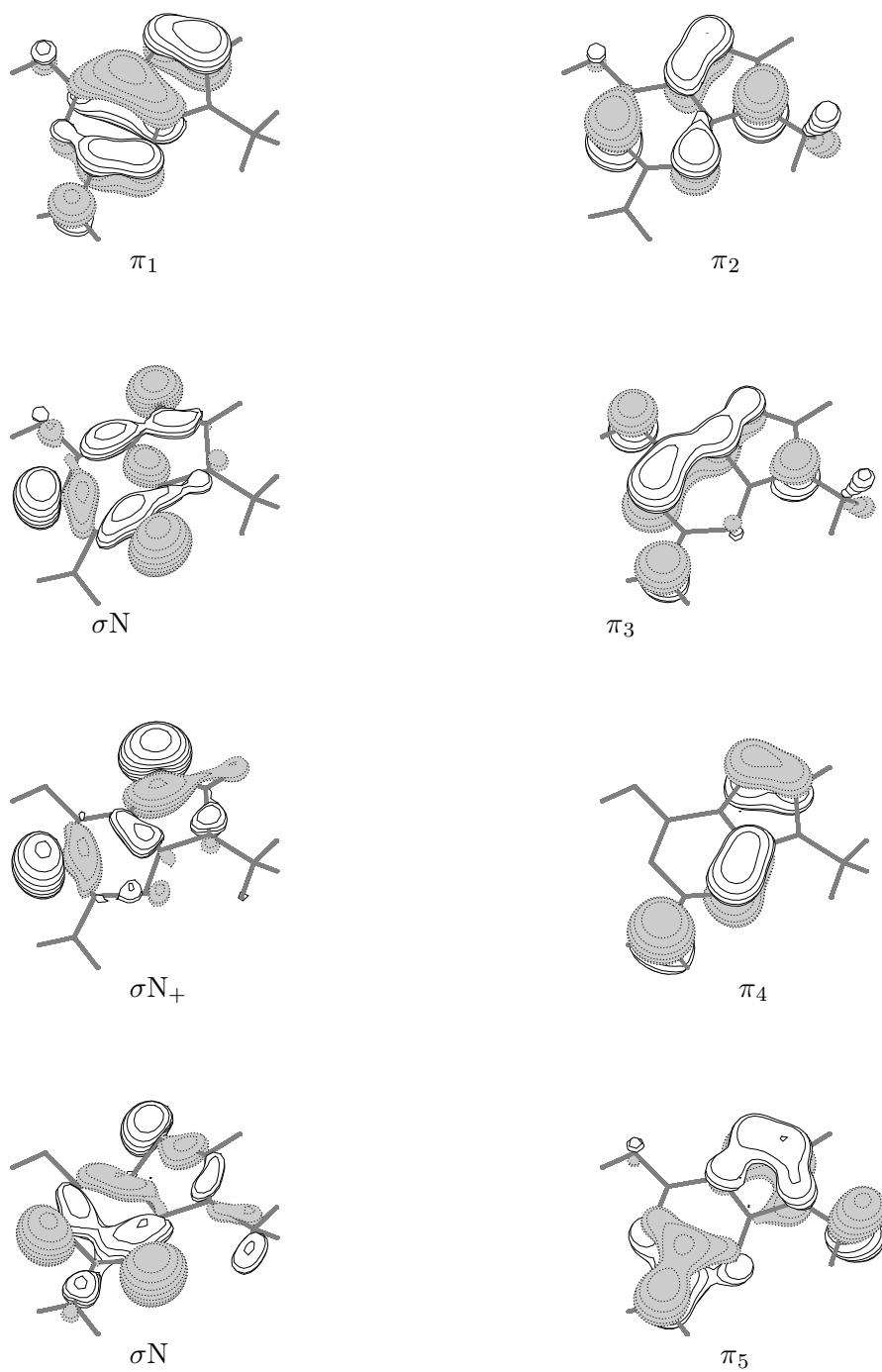


Figure 5.3 Dyson orbitals of the enol form of 9-methylguanine.

Dyson orbitals from one isomer to the other. A higher peak at 10.86 eV, with intensity closer to that of the first one, is assigned to the π_4 hole; the Dyson orbital is approximately conserved after the proton transfer. Note that Koopmans's theorem (KT) results predict the wrong order of states for the enol form. A third σ hole for both isomers is in reasonable agreement with the experimental peak at 11.32 eV. Finally, the feature at 13.3 eV is assigned to the π_5 hole.

The quality of results obtained with the P3/6-311G** model is generally sufficient to assign outer valence photoelectron spectra of typical organic molecules. Only 1s core orbitals are omitted from the self-energy summations of Eq. (3.6). Pole strengths between 0.85 and 0.89 for all states listed here confirm the perturbative arguments on which P3 is based. This kind of calculation can be executed with the standard version of Gaussian 98 [45] by activating certain input keywords [46].

In general, correlation corrections are larger for σ holes than for π holes. It is not unusual for these differential correlation effects to change the predicted order of final states. Heterocyclic organic molecules with nitrogen-centered, nonbonding electrons are not alone in this respect. Organometallics, transition metal complexes, and clusters of metal oxides and metal halides also require this kind of theoretical interpretation.

7. P3 TEST RESULTS

The P3 approximation to the self-energy was applied to the atoms Li through Kr and to neutral and ionic molecular species from the G2 set [47]. For the atoms, a set of 22 representative basis sets was tested. Results for the molecular set were obtained using standard Pople basis sets as described below.

Calculations of ionization energies and electron affinities were performed with a modified development version of Gaussian 99 [48]. Pople and Effective Core Potential (ECP) basis sets are provided in this software [49]. Dunning and Atomic Natural Orbital (ANO) basis sets were obtained from the EMSL Gaussian Basis Set Library [50].

7.1. Atomic Ionization Energies

Atomic calculations are an excellent way to investigate the strengths and weaknesses of a computational procedure's ability to account for electron correlation. Because of the small size of the systems, calculations are sensitive to the theoretical treatment, especially the basis set.

Table 5.4 $4s^n 3d^m$ electron configurations of transition metal atoms.

Atom	Configuration	Multiplicity
Sc	[Ar] $4s^2 3d^1$	2
Ti	[Ar] $4s^2 3d^2$	3
V	[Ar] $4s^2 3d^3$	4
Cr	[Ar] $4s^1 3d^5$	7
Mn	[Ar] $4s^2 3d^5$	6
Fe	[Ar] $4s^2 3d^6$	5
Co	[Ar] $4s^2 3d^7$	4
Ni	[Ar] $4s^2 3d^8$	3
Cu	[Ar] $4s^1 3d^{10}$	2

Fortuitous cancellation of errors is less likely and inherent tendencies of the method under examination may be revealed.

We have performed calculations on the atoms Li through Kr with many basis sets using the P3 method. The results are presented in three groups: alkali and alkaline earth elements, transition metal elements, and p group elements. Electron configurations of transition metal atoms are listed in Table 5.4. For the purposes of this discussion, we have grouped the basis sets into four categories: Pople, Dunning, ECP, and ANO. Data are reported in Tables 5.5, 5.6, and 5.7 for the basis sets that give the best results from each of the four groups. No orbitals were dropped from the summations in the P3 formulae of Eqs. (3.6) and (3.9).

A summary of all calculations is given in Table 5.8. Dunning basis sets are available for p group elements only. Basis set comparisons for other atoms therefore omit this category. Pople bases appear first, followed by the Dunning, ANO, and ECP bases. The mean absolute deviations (MADs) are listed.

P group elements. Molecules with p group elements already have been studied with the P3 approximation and they probably will remain inviting objects of study with this method. Errors obtained for the p group elements (Table 5.5) are somewhat larger than those found for organic molecules. Groups VI and VII are especially problematic.

Results for the other open-shell atoms are encouraging. One would expect the P3 method to be considerably less accurate when an unrestricted Hartree-Fock reference state is used. The lowest MAD for B - Ar obtains with the largest of the Dunning sets examined here, i.e. cc-pVQZ. The 6-311++G(3df,3pd) and well-tempered basis sets (WTBS) are roughly equivalent, with MADs of 0.50 eV and 0.57 eV, respectively.

Table 5.5 Ionization energies and their MADs (eV) computed with the best basis sets for p group elements.

Atom	Pople 6-311++G (3df,3pd)	Dunning cc-pVQZ	ANO WTBS	ECP LANL2DZ	Exp. ^a
B	8.10	8.25	7.72	7.68	8.30
C	10.97	11.15	10.87	10.57	11.26
N	14.18	14.38	14.82	13.78	14.54
O	12.82	13.24	14.05	12.35	14.61
F	16.79	17.13	18.21	16.25	17.42
Ne	21.21	21.46	22.67	20.56	21.56
Al	5.64	5.86	5.34	5.43	5.99
Si	7.77	8.03	7.49	7.77	8.15
P	10.14	10.41	9.96	9.99	10.49
S	9.52	10.08	9.34	9.33	10.36
Cl	12.26	12.74	12.41	12.18	13.01
Ar	15.25	15.65	15.48	15.08	15.75
Ga	5.73		5.45	5.37	6.00
Ge	7.66		7.42	7.34	7.88
As	9.73		9.54	9.43	9.82
Se	8.96		8.87	8.59	9.75
Br	11.26		11.29	10.88	11.84
Kr	13.77		13.87	13.41	14.00
MAD	0.50	0.25	0.57	0.82	

^a Ref. 51.

ECP basis sets performed as expected for these atomic systems, with the Los Alamos double- ζ (LANL2DZ) working best. Its MAD is only 0.82 eV. However, the 31 split-valence ECP of Stevens et al. (CEP-31G) and the Stuttgart-Dresden ECP (SDD) each generated a similar error of 0.87 eV.

It is reasonable to expect P3 calculations with open-shell reference states to be less accurate than their closed-shell counterparts. Unfortunately, there is no obvious correlation between errors and multiplicity.

Errors remain relatively constant for groups III through V, with a sharp increase at group VI. Removal of electrons from β spinorbitals in unrestricted Hartree-Fock reference states is relatively poorly described. Absolute errors for the noble gas elements are significantly lower than

Table 5.6 Ionization Energies and their MADs (eV) computed with the best basis sets for alkali and alkaline earth elements.

Atom	Pople 6-311++G(3df,3pd)	ANO Roos DZ	ECP LANL2DZ	Exp. ^a
Li	5.35	5.36	5.33	5.39
Be	8.81	8.83	8.70	9.32
Na	4.97	4.97	N/A	5.14
Mg	7.24	7.26	N/A	7.64
K	4.22	4.07	3.99	4.34
Ca	5.83	5.84	5.68	6.11
MAD	0.25	0.27	0.37	

^a Ref. 51.

those for groups VI and VII. Multireference character in O and F militates against the P3 approximation,

Alkali and alkaline earth metals. Results obtained for the group I and group II atoms are encouraging. As Table 5.6 shows, calculations for the alkali atoms are slightly more reliable than those for the alkaline earths. The largest error obtains for the quasidegenerate Be atom. ECP bases provide a convenient alternative to all-electron treatments.

First-row transition metals. These metals present formidable challenges for quantum chemistry. With the energies of the *d* orbitals being so close to those of the *s* orbitals for these atoms, the possibility of final states with low pole strengths cannot be ignored. In addition, the middle transition metals are generally difficult to describe with single-determinant methods and require a more advanced approach for a proper description.

In Table 5.7 data are omitted for the Sc and Ti atoms, where pole strengths were well below the acceptable level of 0.80. The remaining results are encouraging. The Roos double- ζ and the ECP SDD sets perform well for Sc through Cr and Ni through Zn. If one ignores the results for Mn through Co, the average absolute error falls sharply to 0.41 eV for the Roos double- ζ basis and to 0.44 eV for the ECP SDD set.

Summary. Despite some noticeable flaws, the performance of the P3 method for atomic calculations is satisfactory. Results for the chalcogens and halogens are somewhat disappointing. In view of the difficulties in describing these atoms with far more complicated methods, this outcome is not surprising. Troublesome results for Mn, Fe, and Co are not

Table 5.7 Ionization energies and their MADs (eV) computed with the best basis sets for transition metal elements.

Atom	Pople 6-31G(d,p)	ANO Roos DZ	ECP SDD	Exp. ^a
Sc		6.32	6.36	6.54
Ti	6.73		6.52	6.80
V	5.09	6.62	6.66	6.74
Cr	5.76	6.44	6.48	6.76
Mn	5.81	5.58	4.58	7.43
Fe	5.92	6.84	6.75	7.90
Co	6.00	6.89	6.87	7.86
Ni	6.07	7.00	6.92	7.63
Cu	6.14	7.10	6.93	7.72
Zn	8.24	8.87	8.64	9.39
MAD	1.73	0.70	0.81	

^a Ref. 51.

unexpected. It is perhaps more surprising that the P3 method performs so well for the remainder of the first-row transition metals.

Aside from the results for the individual atoms, some trends in basis set performance may be observed. Pople basis sets produced results that were fairly accurate, especially for alkali and alkaline earth metals. Although the results are much less accurate for the *p* group elements, they are certainly within acceptable error for this simple approximation. The steady decrease in errors observed in the progression from the P3/6-31G to the P3/6-311++G(3df,3pd) level for nontransition elements also attests to the sound design of these basis sets.

The Pople basis sets are perhaps the most efficacious for general applications. Since the integral package in the Gaussian suite of programs is especially efficient with these basis sets, large systems may be tackled routinely in this manner. The Roos double- ζ basis set provides excellent results for all of the elements studied here, including the transition metals. As the Roos triple- ζ basis requires a significant increase in computational cost, this choice is best for smaller systems.

Dunning basis sets have been optimized with atomic configuration interaction calculations and show steady improvement as the basis set quality is increased. The cc-pVQZ set is the most accurate in this category, but its size probably will preclude its use in the larger calculations

Table 5.8 Mean absolute deviations (eV) in the computed ionization energies.

Basis set ^a	Alkali and alkaline earths	<i>P</i> group elements	Transition metals
6-31G	0.41	0.92	2.78
6-311G	0.33	0.83	1.99
6-311++G	0.33	0.80	1.78
6-31G(d,p)	0.33	0.66	1.73
6-311++G(3df,3pd)	0.25	0.50	1.93
cc-pVDZ		0.67	
aug-cc-pVDZ		0.51	
cc-pVTZ		0.37	
aug-cc-pVTZ		0.31	
cc-pVQZ		0.25	
WTBS	0.40	0.57	2.67
Wachters			1.47
Ahlrichs	0.46	1.31	1.91
Roos DZ	0.27	0.45	0.70
Roos TZ	0.38	0.13	
CEP-121G		0.91	0.94
CEP-31G		0.87	0.97
CEP-4G		0.67	0.97
LANL2DZ	0.37	0.82	1.91
LANL2MB	0.78	1.48	1.58
SDD	0.63	0.87	0.81
SHC	0.34	0.90	

^a Refs. 49 and 50.

for which the P3 method is most suited. A steady decline in MAD occurs with increasing size of Dunning basis sets.

Among the ANO basis sets, the Roos double- ζ basis set is clearly preferable. Convergence problems were encountered with Roos triple- ζ basis sets, especially during the pole search in the propagator calculation. Preliminary results are encouraging.

The performance of the P3 method used in conjunction with ECPs is also encouraging. Among the *p* group metals, the CEP-4G set is the most accurate (MAD of 0.67 eV), with the SHC potential of Goddard and Smedley performing best for the alkalis and alkaline earths (MAD of 0.34 eV). The SDD sets succeed in all three cases and produce errors that are competitive with all of the other ECPs.

The overall performance of the P3 method for the atomic systems (see Table 5.8) is encouraging. Transition metals are difficult to describe

and the average absolute error for these atoms is generally several times larger than that obtained for the other atoms in the study. However, an unexpected result is the ability of the ECP basis sets to generate errors of less than 1.0 eV for most atoms. Although the errors are relatively large, we anticipate that a combination of ECP and all-electron basis sets will provide an acceptable description of molecules containing these atoms.

7.2. Molecular Species

The G2 set. Calculations of ionization energies and electron affinities for molecules and ions from the G2 set [47] were performed with P3 methods. The diversity of bonding in this set presents a convenient standard for testing the new methodology introduced here, such as electron affinity formulae and procedures for electron binding energies of open-shell systems.

Our implementation computes only vertical ionization energies and electron affinities, but experimental results for the G2 species are adiabatic. To facilitate a direct comparison between the theoretical and experimental results, it is necessary that either the theoretical results be corrected to adiabatic values or that the adiabatic values be related to vertical ones. We have chosen the latter approach and have corrected the experimental results with computational data.

Electron binding energies were calculated in three ways, each involving four steps. The complete procedure is outlined below.

A. Neutral Geometry:

1. HF/6-31G(d) geometry optimization for neutral species with vibrational frequencies to determine zero-point energy.
2. MP2/6-31G(d) geometry optimization for neutral species.
3. Electron propagator calculations
 - a) Calculation of electron affinity of the neutral species using the P3 method with 6-311++G(2df,2p) basis set.
 - b) Calculation of ionization energy of the neutral species using the P3 method with 6-311G(2df,2p) basis set.
4. Single point energies
 - a) Single-point MP2/6-31G(d) calculation for the anionic species at the neutral geometry.
 - b) Single-point MP2/6-31G(d) calculation for the cationic species at the neutral geometry.

B. Anion Geometry:

1. HF/6-31G(d) geometry optimization for anionic species with vibrational frequencies to determine the zero-point energy.
2. MP2/6-31G(d) geometry optimization for anionic species.
3. Calculation of ionization energy (electron detachment energy) of the anionic species using P3 method with 6-311++G(2df,2p) basis set.
4. Single-point MP2/6-31G(d) calculation for the neutral species at the anion geometry.

C. Cation Geometry:

1. HF/6-31G(d) geometry optimization for cationic species with vibrational frequencies to determine the zero-point energy.
2. MP2/6-31G(d) geometry optimization for cationic species.
3. Calculation of electron affinities of the cationic species using P3 method with 6-311G(2df,2p) basis set.
4. Single-point MP2/6-31G(d) calculation for the neutral species at the cation geometry.

In cases where experimental data were missing for ionization energies or electron affinities, some steps were omitted. The initial geometries were obtained from the authors of the original G2 study [52].

Transition energies between cations and neutral species were calculated by two procedures. In the first one, the vertical ionization energy of the neutral molecule was determined with the P3 method. These values were compared with experimental adiabatic ionization energies of the neutral molecules, which were adjusted according to

$$\text{IE}_N = \text{IE}_{\text{exp}} + Z_N + R_{N-1} - Z_{N-1}, \quad (7.1)$$

where IE_{exp} is the experimental (adiabatic) ionization energy, Z_N is the zero-point energy (ZPE) of the neutral molecule calculated at the HF/6-31G(d) level, Z_{N-1} is the ZPE of the cation, and R_{N-1} is the relaxation energy of the cation between the neutral and cation equilibrium geometries. In other words, each standard of comparison IE_N is an experimental datum adjusted by calculated zero-point and relaxation energies. In the second procedure, the vertical electron affinity of the cation formed in the first case was computed with the P3 method. These values were compared with experimental, adiabatic electron affinities of the cation (i.e. IE_{exp}), which were adjusted according to

$$\text{EA}_{N-1} = \text{IE}_{\text{exp}} + Z_N - R_N - Z_{N-1}, \quad (7.2)$$

where EA_{N-1} is the value to which the P3 result is compared.

Transitions between anions and neutral species were also calculated with two procedures. In the first, we calculated the vertical P3 electron affinities of neutral species. The experimental adiabatic electron affinities of the neutral molecules were shifted according to

$$EA_N = EA_{\text{exp}} - Z_N - R_{N+1} + Z_{N+1}, \quad (7.3)$$

where EA_{exp} is the experimental (adiabatic) electron affinity, Z_N is the ZPE of the neutral molecule, Z_{N+1} is the ZPE of the anion, and R_{N+1} is the relaxation energy of the anion between the neutral and anion equilibrium geometries. In the second procedure, the P3 ionization energy of the anion (that is, the anion's electron detachment energy) was calculated at the anion's geometry. Vertical ionization energies of the anions IE_{N+1} were obtained from experimental adiabatic values, where

$$IE_{N+1} = EA_{\text{exp}} + Z_{N+1} + R_N - Z_N. \quad (7.4)$$

This sequence of calculations was applied to neutral and ionic molecular species from the G2 test set. Experimental adiabatic electron affinities and ionization energies were taken from Refs. 53 - 74.

Neutral singlets. This class of systems comprises singlet molecules with transitions to doublet cations or anions. Most applications of the P3 method will pertain to such systems.

Electron affinities were calculated as described above with the vertical corrections applied to the experimental results. For molecules with electron affinity data, the overall results are good, with a MAD of just 0.20 eV. The F atom was difficult to describe and this failure is probably related to the low accuracy of the CF_2 calculation, where the error exceeded 1.0 eV.

Similar accuracy obtains when considering the ionization energy (i.e. the electron detachment energy) of the associated doublet anions. Here, MAD is 0.33 eV. For anionic ozone, the error is significantly larger. It is well known that ozone has a great deal of multireference character in its ground state. Ozone therefore is a poor candidate for the P3 method, which relies on the qualitative validity of the single-reference description.

Next we consider ionization energies of neutral singlet states and electron affinities of the associated doublet cations. Here we find that the overall error is slightly larger (MAD of 0.36 eV) than was the case for the electron affinities. Electron affinities of the doublet cations are not treated as well by the P3 method. Here MAD is 0.52 eV.

Neutral doublet states. Electron affinities of neutral doublets where the corresponding anions are singlets, not triplets, are poorly calculated

Table 5.9 MADs for G2 molecules and ions.

Initial geometry	Final state	MAD (eV)	n ^a
¹ M	² M ⁻	0.20	10
² M ⁻	¹ M	0.33	
¹ M	² M ⁺	0.36	35
² M ⁺	¹ M	0.52	
² M	¹ M ⁻	1.11	24
¹ M ⁻	² M	0.20	
² M	¹ M ⁺	0.26	10
¹ M ⁺	² M	0.21	

^a Number of species [75].

with the P3 method. For these systems, MAD is 1.11 eV. Evaluation of the vertical electron detachment energies of the singlet anions, however, is a more effective approach, for MAD is only 0.20 eV.

For the case of doublet neutrals and associated singlet cations, the ionization energy results are good. Here, the average absolute error is only 0.26 eV. Electron affinities for the singlet cations are also rather accurate. MAD is even less, i.e. 0.21 eV. For energy differences between doublets and triplets, there are not enough systems to establish patterns. These results are highly variable in quality.

Doublet reference states. Some patterns emerge from the calculations with doublet reference states. Table 5.9 presents a summary of all cases involving transitions between singlets and doublets. Ionization energy calculations perform well when a doublet reference state is used. However, electron affinity calculations are advisable only when the doublet reference state is cationic. Even here, it is preferable to reverse the roles of initial and final states by choosing the closed-shell neutral as the reference state in an ionization energy calculation. The P3 method is not suitable for attachment of an electron to a neutral doublet reference state to form a closed-shell anion. It is preferable to choose the anion as the reference state for a P3 calculation of an electron detachment energy. Results for triplets are unpredictable at best.

8. CONCLUSIONS AND PROSPECTUS

P3 calculations with unrestricted Hartree-Fock reference states have been reported here for the first time. In addition, a P3 procedure for electron affinities of closed-shell and open-shell systems has been presented.

Some general trends may be discerned in the P3 results on atoms. Ionization energies involving high-spin states are described well with Pople, Dunning, ANO, and ECP basis sets. Average errors for the p block elements are between 0.25 eV for Dunning's quadruple- ζ basis and 0.82 eV for the LANL double- ζ set. For the alkali and alkaline earth metals, the average errors are smaller. Transition metals in the fourth period require use of ANO or SDD sets; the average errors are 0.7 - 0.8 eV. Despite the complex character of electron correlation in $2p$ and $3d$ elements, reasonable results obtain for this simple electron propagator approximation based on an unrestricted Hartree-Fock reference state. For transition metal complexes with high oxidation states and highly electronegative ligands, one may expect the errors for metal-centered holes to be smaller. Results of test calculations using SDD ECPs are especially encouraging for this class of molecules, especially if a closed-shell reference state may be used. Larger errors may be expected for late transition metals, low oxidation states, and relatively electropositive ligands. The P3 method may be used to aid state assignments in photoelectron spectra of organometallics.

Results on molecules and molecular ions display some instructive tendencies. Electron detachment energies from closed-shell reference states (neutral or anionic) are treated well if there is little multiconfigurational character in the initial singlet. Average errors for these cases are about 0.2 - 0.4 eV. The quality of electron attachment energies to closed-shell species is better, especially if the singlet is cationic. Another new class of P3 calculations makes use of unrestricted Hartree-Fock reference states. If the reference state is a doublet, electron detachment energies are treated well, with average errors of 0.2 - 0.3 eV. Electron attachment energies to doublets are satisfactory if the reference state is cationic; caution must be exercised if the doublet reference state is neutral.

Although P3 procedures perform well for a variety of atomic and molecular species, caution is necessary when applying this method to open-shell reference states. Systems with broken symmetry in unrestricted Hartree-Fock orbitals should be avoided. Systems with high multireference character are unlikely to be described well by the P3 or any other diagonal approximation. In such cases, a renormalized elec-

tron propagator should be used. In general, P3 will fail when Hartree-Fock theory does not provide a qualitatively acceptable description of the reference state.

The pole strength is a useful diagnostic criterion of problematic cases. Close agreement with experiment in the presence of a pole strength that is less than 0.80 is likely to be the result of a fortuitous cancellation of errors.

The P3 methods for ionization energies and electron affinities provide useful, correlated corrections to canonical Hartree-Fock orbital energies. Their computational demands are modest, especially for electron detachment energies. It is often possible to avoid difficult cases by reversing the labels of initial and final states. Fifth-power arithmetic scaling factors characterize the bottleneck contractions in P3 calculations. Full integral transformations to the Hartree-Fock basis and storage of the largest blocks of integrals may be avoided. In general, P3 calculations may be executed for any molecule where a second-order total energy calculation is feasible. Information on excited final states may be obtained easily. Interpretation of the results in terms of orbitals is facilitated by the diagonal self-energy approximation, where each Dyson orbital is equal to a canonical Hartree-Fock orbital times a scaling factor which is equal to the square root of the corresponding pole strength.

ACKNOWLEDGEMENTS

We thank Dr. Yasuteru Shigeta for informative conversations and assistance in the preparation of this manuscript. This work was supported by the National Science Foundation under grant CHE-9873897 and by the Kansas DEPSCoR program.

REFERENCES

1. J. Linderberg and Y. Öhrn, *Propagators in Quantum Chemistry* (Academic Press, New York, 1973).
2. B. T. Pickup and O. Goscinski, *Mol. Phys.* **26**, 1013 (1973).
3. L. S. Cederbaum and W. Domcke, *Adv. Chem. Phys.* **36**, 206 (1977).
4. J. Simons, *Annu. Rev. Phys. Chem.* **28**, 1 (1977).
5. J. Simons, *Theor. Chem. Adv. Persp.* **3**, 1 (1979).
6. M. F. Herman, K. F. Freed, and D. L. Yeager, *Adv. Chem. Phys.* **48**, 1 (1981).
7. Y. Öhrn and G. Born, *Adv. Quant. Chem.* **13**, 1 (1981).

8. W. von Niessen, J. Schirmer and L. S. Cederbaum, *Comput. Phys. Rep.* **1**, 57 (1984).
9. J. V. Ortiz in *Computational Chemistry: Reviews of Current Trends*, Vol. 2, J. Leszczynski, ed. (World Scientific, Singapore, 1997) p. 1.
10. J. V. Ortiz in *Conceptual Perspectives in Quantum Chemistry*, Vol. 3, J.-L. Calais and E. Kryachko, eds. (Kluwer, Dordrecht, 1997) p. 465.
11. J. V. Ortiz *Adv. Quantum Chem.* **35**, 33 (1999).
12. J. V. Ortiz, *J. Chem. Phys.* **104**, 7599 (1996).
13. J. V. Ortiz and V. G. Zakrzewski, *J. Chem. Phys.* **105**, 2762 (1996).
14. V. G. Zakrzewski, and J. V. Ortiz, *J. Phys. Chem.* **100**, 13979 (1996).
15. V. G. Zakrzewski, O. Dolgounitcheva, and J. V. Ortiz, *J. Chem. Phys.* **105**, 8748 (1996).
16. V. G. Zakrzewski and J. V. Ortiz, *J. Mol. Struct. (Theochem)* **388**, 351 (1996).
17. J. V. Ortiz, *Int. J. Quantum Chem.* **63**, 291 (1997).
18. M. Enlow, J.V. Ortiz and H.P. Lüthi, *Molecular Physics* **92**, 441 (1997).
19. O. Dolgounitcheva, V. G. Zakrzewski, and J. V. Ortiz, *Int. J. Quantum Chem.* **65**, 463 (1997).
20. O. Dolgounitcheva, V. G. Zakrzewski, and J. V. Ortiz, *J. Phys. Chem. A* **101**, 8554 (1997).
21. V. G. Zakrzewski, O. Dolgounitcheva, and J. V. Ortiz, *J. Chem. Phys.* **107**, 7906 (1997).
22. O. Dolgounitcheva, V. G. Zakrzewski, and J. V. Ortiz, *J. Chem. Phys.* **109**, 87 (1998).
23. O. Dolgounitcheva, V. G. Zakrzewski, and J. V. Ortiz, *Int. J. Quantum Chem.* **70**, 1037 (1998).
24. V. G. Zakrzewski, O. Dolgounitcheva, and J. V. Ortiz, *Int. J. Quantum Chem.* **75**, 607 (1999).
25. O. Dolgounitcheva, V. G. Zakrzewski, and J. V. Ortiz, *Int. J. Quantum Chem.* **80**, 831 (2000).
26. O. Dolgounitcheva, V. G. Zakrzewski, and J. V. Ortiz, *J. Phys. Chem. A* **104**, 10032 (2000).
27. O. Dolgounitcheva, V. G. Zakrzewski, and J. V. Ortiz, *J. Amer. Chem. Soc.* **122**, 12304 (2000).
28. J. M. Herbert and J. V. Ortiz, *J. Phys. Chem.* **A104**, 11786 (2000).
29. H. Hopper, M. Lococo, O. Dolgounitcheva, V. G. Zakrzewski, and J. V. Ortiz, *J. Amer. Chem. Soc.* **122**, 12813 (2000).
30. V. G. Zakrzewski, O. Dolgounitcheva, and J. V. Ortiz, *Int. J. Quant. Chem.* **75**, 607 (1999).
31. V. G. Zakrzewski, J. V. Ortiz, J. A. Nichols, D. Heryadi, D. L. Yeager, and J. T. Golab, *Int. J. Quant. Chem.* **60**, 29 (1996).
32. J. Simons and W. D. Smith, *J. Chem. Phys.* **58**, 4899 (1973).
33. G. D. Purvis and Y. Öhrn, *Chem. Phys. Lett.* **33**, 396 (1975).

34. L. S. Cederbaum, W. Domcke, J. Schirmer, and W. von Niessen, *Adv. Chem. Phys.* **65**, 115 (1986).
35. J. V. Ortiz, *J. Chem. Phys.* **108**, 1008 (1998).
36. O. Dolgounitcheva, V. G. Zakrzewski, and J. V. Ortiz, *J. Chem. Phys.* **114**, 130 (2001).
37. J. T. Golab and D. L. Yeager, *J. Chem. Phys.* **87**, 2925 (1987).
38. D. Heryadi and D. L. Yeager, *J. Chem. Phys.* **114**, 5124 (2001).
39. J. V. Ortiz, *J. Chem. Phys.* **109**, 5741 (1998).
40. J. V. Ortiz, *Int. J. Quant. Chem.* **70**, 651 (1998).
41. J. V. Ortiz, *Chem. Phys. Lett.* **296**, 494 (1998).
42. J. V. Ortiz, *Int. J. Quant. Chem.* **75**, 615 (1999).
43. J. V. Ortiz, *Chem. Phys. Lett.* **297**, 193 (1998).
44. J. Lin, C. Yu, S. Peng, I. Akiyama, K. Li, L. K. Lee, and P. R. Lebreton, *J. Phys. Chem.* **84**, 1006 (1980).
45. GAUSSIAN 98 (Revision A8), M. J. Frisch, G. W. Trucks, H. B. Schlegel, G. E. Scuseria, M. A. Robb, J. R. Cheeseman, V. G. Zakrzewski, J. A. Montgomery, Jr., R. E. Stratmann, J. C. Burant, S. Dapprich, J. M. Millam, A. D. Daniels, K. N. Kudin, M. C. Strain, O. Farkas, J. Tomasi, V. Barone, M. Cossi, R. Cammi, B. Mennucci, C. Pomelli, C. Adamo, S. Clifford, J. Ochterski, G. A. Petersson, P. Y. Ayala, Q. Cui, K. Morokuma, D. K. Malick, A. D. Rabuck, K. Raghavachari, J. B. Foresman, J. Cioslowski, J. V. Ortiz, B. B. Stefanov, G. Liu, A. Liashenko, P. Piskorz, I. Komaromi, R. Gomperts, R. L. Martin, D. J. Fox, T. Keith, M. A. Al-Laham, C. Y. Peng, A. Nanayakkara, C. Gonzalez, M. Challacombe, P. M. W. Gill, B. Johnson, W. Chen, M. W. Wong, J. L. Andres, M. Head-Gordon, E. S. Replogle, and J. A. Pople, Gaussian, Inc., Pittsburgh PA, 1998.
46. Contact J. V. Ortiz at ortiz@ksu.edu for specific information.
47. L. A. Curtiss, P. C. Redfern, K. Raghavachari, and J. A. Pople, *J. Chem. Phys.* **109**, 42 (1998).
48. GAUSSIAN 99, DEVELOPMENT VERSION (REVISION B.06+), M. J. Frisch, G. W. Trucks, H. B. Schlegel, G. E. Scuseria, M. A. Robb, J. R. Cheeseman, V. G. Zakrzewski, J. A. Montgomery, Jr., R. E. Stratmann, J. C. Burant, S. Dapprich, J. M. Millam, A. D. Daniels, K. N. Kudin, M. C. Strain, O. Farkas, J. Tomasi, V. Barone, B. Mennucci, M. Cossi, C. Adamo, J. Jarmillo, R. Cammi, C. Pomelli, J. Ochterski, G. A. Petersson, P. Y. Ayala, K. Morokuma, D. K. Malick, A. D. Rabuck, K. Raghavachari, J. B. Foresman, J. V. Ortiz, Q. Cui, A. G. Baboul, S. Clifford, J. Cioslowski, B. B. Stefanov, G. Liu, A. Liashenko, P. Piskorz, I. Komaromi, R. Gomperts, R. L. Martin, D. J. Fox, T. Keith, M. A. Al-Laham, C. Y. Peng, A. Nanayakkara, M. Challacombe, P. M. W. Gill, B. Johnson, W. Chen, M. W. Wong, J. L. Andres, C. Gonzalez, M. Head-Gordon, E. S. Replogle, and J. A. Pople, Gaussian, Inc., Pittsburgh PA, 1998.
49. Basis sets (excluding the ANO category) are specified according to the Gaussian 98 keyword used to invoke their use. See A. Frisch and M. J. Frisch, *Gaussian 98 User's Reference* (Gaussian, Inc., Pittsburgh, 1998) pp. 25-28 and references therein for a complete description of these basis sets.
50. Additional basis sets were obtained from the Extensible Computational Chemistry Environment Basis Set Database, June 26, 2000 Version, as developed and

distributed by the Molecular Science Computing Facility, Environmental and Molecular Sciences Laboratory, which is part of the Pacific Northwest Laboratory, P.O. Box 999, Richland, Washington 99352, USA, and is funded by the U.S. Department of Energy. The Pacific Northwest Laboratory is a multiprogram laboratory operated by Battelle Memorial Institute for the U.S. Department of Energy under contract DE-AC06-76RLO 1830.

51. C. E. Moore, *National Standard Reference Data Series 34* (U.S. Government Printing Office, Washington, D.C., 1970).
52. Information on G2 calculations for ionization energies and electron affinities was obtained from the following URL: <http://chemistry.anl.gov/compmat/comptherm.htm>
53. J. A. Pople, M. Head-Gordon, D. J. Fox, K. Raghavachari, and L. A. Curtiss, *J. Chem. Phys.* **90**, 5622 (1989).
54. L. A. Curtiss, C. Jones, G. W. Trucks, K. Raghavachari, and J. A. Pople, *J. Chem. Phys.* **93**, 2537 (1990).
55. J. Berkowitz, G. B. Ellison, and D. Guttman, *J. Phys. Chem.* **78**, 2744 (1994).
56. H. Hotop and W. C. Lineberger, *J. Phys. Chem. Ref. Data* **14**, 731 (1985).
57. D. W. Arnold, S. E. Bradforth, T. N. Kitsopoulos, and D. M. Neumark, *J. Chem. Phys.* **95**, 8753 (1991).
58. B. Ruscic and J. Berkowitz, *J. Chem. Phys.* **95**, 4033 (1991).
59. K. K. Murray, D. G. Leopold, T. M. Miller, and W. C. Lineberger, *J. Chem. Phys.* **89**, 5442 (1988).
60. S. E. Bradforth, E. H. Kim, D. W. Arnold, and D. M. Neumark, *J. Chem. Phys.* **98**, 800 (1993).
61. K. M. Ervin, J. Ho, and W. C. Lineberger, *J. Phys. Chem.* **92**, 5405 (1988).
62. S. G. Lias, J. E. Bartmess, J. E. Liebman, J. L. Holmes, R. D. Levin, and W. G. Mallard, *J. Phys. Chem. Ref. Data Suppl.* **1**, 17 (1988).
63. M. K. Gilles, M. L. Polak, and W. C. Lineberger, *J. Chem. Phys.* **96**, 8012 (1992).
64. M. K. Gilles, K. M. Ervin, J. Ho, and W. C. Lineberger, *J. Phys. Chem.* **96**, 1130 (1992).
65. H. W. Sarkas, J. H. Hendricks, S. T. Arnold, and K. H. Bowen, *J. Chem. Phys.* **100**, 1884 (1994).
66. J. M. Oakes, L. B. Harding, and G. B. Ellison, *J. Chem. Phys.* **83**, 5400 (1985).
67. *Handbook of Chemistry and Physics*, edited by D. R. Lide (CRC, Boca Raton, 1996).
68. B. Ruscic and J. Berkowitz, *J. Chem. Phys.* **98**, 2568 (1993).
69. B. Ruscic, E. H. Appelman, and J. Berkowitz, *J. Chem. Phys.* **95**, 7957 (1991).
70. R. J. Lipert and S. D. Coulson, *J. Chem. Phys.* **92**, 3240 (1990).
71. B. Ruscic and J. Berkowitz, *J. Chem. Phys.* **95**, 4378 (1991).
72. J. Berkowitz, E. H. Appelman, and W. A. Chupka, *J. Chem. Phys.* **58**, 1950 (1973).
73. B. Ruscic and J. Berkowitz, *J. Chem. Phys.* **95**, 2407 (1991).
74. B. Ruscic and J. Berkowitz, *J. Chem. Phys.* **95**, 2416 (1991).

75. Singlet electron affinities: H_2CCC , O_3 , HNO , LiH , SO_2 , S_2O , HCF , CF_2 , CH_2S , SiH_2 . Singlet ionization energies: HF , H_2O , Si_2H_6 , HCl , H_2S , cyclopropene, CS , CO_2 , ClF , CS_2 , thiooxirane, Si_2H_2 , propyne, SiH_4 , Si_2H_4 , PH_3 , N_2H_2 , HOF , NH_3 , C_2H_2 , BF_3 , B_2F_4 , BCl_3 , B_2H_4 , CH_3CHO , CH_3SH , CH_3OH , NCCN , CO , CH_4 , CH_3F , CH_3Cl , CF_2 , CH_2S , SiH_2 . Doublet electron affinities: HCCO , HCO , HOO , NCO , NO_2 , OF , CH_3O , NH_2 , CH_2CN , CH_2NC , C_2H_3 , C_3H_5 , CCH , $\text{CH}_3\text{CH}_2\text{O}$, CH_3S , H_2CCCH , H_2CCHO , CH_3CO , CH_3 , CN , OH , PH_2 , SH , SiH_3 . Doublet ionization energies: Si_2H_5 , CH_2SH , C_2H_5 , H_2COH , N_2H_3 , CH_3 , CN , NH_2 , PH_2 , SiH_3 .